



**HAL**  
open science

## Revisiting the methods of determining hydraulic conductivity of saturated expansive clays in low-compressibility zone

Wei Su, Yu-Jun Cui, Feng Zhang, Weimin Ye

► **To cite this version:**

Wei Su, Yu-Jun Cui, Feng Zhang, Weimin Ye. Revisiting the methods of determining hydraulic conductivity of saturated expansive clays in low-compressibility zone. *Journal of Rock Mechanics and Geotechnical Engineering*, 2020, 12 (5), pp.1131-1136. 10.1016/j.jrmge.2020.01.004 . hal-03045843

**HAL Id: hal-03045843**

<https://enpc.hal.science/hal-03045843v1>

Submitted on 17 Oct 2022

**HAL** is a multi-disciplinary open access archive for the deposit and dissemination of scientific research documents, whether they are published or not. The documents may come from teaching and research institutions in France or abroad, or from public or private research centers.

L'archive ouverte pluridisciplinaire **HAL**, est destinée au dépôt et à la diffusion de documents scientifiques de niveau recherche, publiés ou non, émanant des établissements d'enseignement et de recherche français ou étrangers, des laboratoires publics ou privés.



Distributed under a Creative Commons Attribution - NonCommercial 4.0 International License

1     **Revisiting the methods of determining hydraulic conductivity of saturated expansive**  
2                                   **clays in low-compressibility zone**

3  
4  
5  
6  
7  
8  
9  
10  
11  
12  
13  
14  
15  
16  
17  
18  
19  
20  
21  
22  
23  
24  
25  
26  
27  
28  
29

Wei SU<sup>1,2</sup>, Yujun CUI<sup>2</sup>, Feng ZHANG<sup>2</sup>, Weimin YE<sup>1</sup>

<sup>1</sup> Key Laboratory of Geotechnical and Underground Engineering of Ministry of Education, Tongji University, Shanghai 200092, China

<sup>2</sup> Ecole des Ponts ParisTech, UR Navier/CERMES, 6-8, av. Blaise Pascal, Cité Descartes, 77455 Marne-la-Vallée, France

**Corresponding author:**

Prof. Yu-Jun CUI  
Ecole des Ponts ParisTech  
6-8 av. Blaise Pascal, Cité Descartes, Champs-sur-Marne  
77455 Marne-la-Vallée cedex 2  
France  
Email: [yu-jun.cui@enpc.fr](mailto:yu-jun.cui@enpc.fr)  
Phone: +33 1 64 15 35 50

## **Abstract**

The hydraulic conductivity of saturated clays is commonly determined either directly by monitoring water flux or indirectly based on Terzaghi's consolidation equation. Similar results are often obtained from the two methods; but sometimes there is significant difference between the two, in particular for expansive soils. In this study, the hydraulic conductivities determined by the two methods are first compared based on existing data in the literature. The indirect method is then revisited attempting to explain the difference identified. A modified effective stress, considering physic-chemical interaction between face-to-face oriented particles, is finally introduced to better describe the compressibility of expansive clays and to further improve the indirect method in determining hydraulic conductivity of such soils in the low-compressibility zone. Extra tests were performed on Gaomiaozi (GMZ) bentonite slurry and the results obtained allowed the modified indirect method to be verified.

**Keywords:** expansive clays; laboratory tests; hydraulic conductivity; Terzaghi's consolidation equation; modified effective stress

## Notation

$c_v$ : consolidation coefficient

$m_v$ : coefficient of compressibility

$m_v'$ : modified coefficient of compressibility

$\gamma_w$ : unit weight of water

$e$ : void ratio

$\sigma'$ : effective stress

$\sigma_v$ : vertical total stress

$\sigma_v'$ : vertical effective stress

$\sigma_s$ : mineral to mineral contact stress

$R$ : total interparticle repulsion divided by total interparticle area

$A$ : total interparticle attraction divided by total interparticle area

$\sigma$ : average net repulsive force acting on the bound water-film area divided by the total cross-sectional area

$\sigma^{R-A}$ : net stress acting on water-films between clay particles

$P_s$ : swelling pressure

$k$ : hydraulic conductivity

$k_d, k_{ind}$ : hydraulic conductivity determined directly and indirectly

$k_{ind}'$ : hydraulic conductivity calculated using modified effective stress

## 1 **Introduction**

2 The hydraulic conductivity  $k$  is one of the key parameters in geotechnical and geo-  
3 environmental engineering. Many efforts have been devoted to the measurement of this  
4 parameter in both field and laboratory conditions. In the laboratory, the hydraulic conductivity  
5 is commonly determined either directly by monitoring water flux or indirectly based on  
6 Terzaghi's consolidation equation. Tavenas et al. (1983) compared the direct and indirect  
7 measurement methods for natural clays and observed that the indirect method overestimated  
8 the values at relatively large void ratios while underestimated the values at smaller void ratios.  
9 The authors attributed the difference to the adopted assumptions of constant  $k$ , compressibility  
10 and coefficient of consolidation during each consolidation stage, as well as the ways of  
11 interpreting the consolidation-time curves on the basis of Terzaghi's consolidation theory.  
12 Mesri et al. (1994) reported that the indirect method typically underestimates the value of  
13 permeability by a factor of 2. Therefore, in the estimation of the settlement of Kansai  
14 International Airport Islands, the values of hydraulic conductivity of the involved Holocene  
15 marine clay determined by the indirect method were multiplied by 2 (Mesri and Funk, 2015).

16  
17 This paper aims at better clarifying the indirect method of determining the hydraulic  
18 conductivity of expansive clays. First, reported  $k$  data for remoulded, undisturbed and  
19 compacted clayey soils, determined directly and indirectly in one-dimensional condition were  
20 collected. Then, the parameters used for indirectly determining  $k$  were analysed one by one in  
21 order to better understand the difference between the direct and the indirect methods. Thereby,  
22 the significance of physico-chemical effects between the bound water around clay particles in  
23 controlling the response of dense clay to external loading was identified. A modified effective  
24 stress concept based on this was postulated and introduced in the Terzaghi's consolidation  
25 theory, aiming to narrow the difference between the direct and the indirect methods. Finally,  
26 the modified method was verified based on existing data from the literature and complementary

27 data from tests on GMZ bentonite. This study suggests the necessity of introducing the modified  
28 effective stress concept into the Terzaghi's consolidation theory for active expansive clays in  
29 the low-compressibility zone.

### 30 **Direct and indirect methods for $k$ determination**

31 Generally, in a conventional step-loading oedometer test,  $k$  can be indirectly calculated at each  
32 loading step based on Terzaghi's consolidation theory as follows:

$$33 \quad k = c_v m_v \gamma_w \quad (1)$$

34 where,  $k$  is the hydraulic conductivity (m/s),  $c_v$  is the consolidation coefficient ( $\text{m}^2/\text{s}$ ),  $m_v$  is the  
35 coefficient of compressibility ( $\text{kPa}^{-1}$ ),  $\gamma_w$  is the unit weight of water (taken equal to  $10 \text{ kN/m}^3$  in  
36 this study).

37

38 Parameter  $c_v$  reflects the rate at which a saturated clay undergoes consolidation when subjected  
39 to an incremental load. In practice, the methods proposed by Casagrande and Fadum (1944)  
40 and Taylor (1948) are routinely used to estimate the  $c_v$  from the settlement-time curve at each  
41 loading step. It appears that this parameter shows mineral-dependence and varies with the stress  
42 state of soil (Retnamony et al., 1998; Sridharan and Nagaraj, 2004).

43

44 At the end of a loading step  $i$ , with corresponding void ratio  $e$ ,  $m_v$  can be determined as follows:

$$45 \quad m_{v,i} = \frac{\Delta e_i}{\Delta \sigma'_{v,i} (1 + e_{i-1})} \quad (2)$$

46 Obviously, any factors involved in the determination of soil deformation and vertical effective  
47 stress increment  $\Delta \sigma'_v$  can influence the value of  $m_v$ .

48

49 Meanwhile, at the end of each consolidation stage, the hydraulic conductivity  $k$  can be  
50 determined directly based on Darcy's law by connecting the base of the soil specimen to a  
51 burette using falling head method or to a pressure/volume controller using constant head  
52 method (ASTM D5856; ASTM D7100).

### 53 Comparison of the two methods based on the literature data

54 In this section, the direct and indirect results reported in the literature are collected and  
55 compared. The sources of data are summarized in Table 1. The reliability of indirect  $k$  values  
56 is evaluated by the ratio  $k_d/k_{ind}$ , where  $k_d$  and  $k_{ind}$  are the direct and indirect hydraulic  
57 conductivities, respectively. The  $k_d/k_{ind}$  results in the high-compressibility zone are plotted in  
58 Fig. 1, together with the  $e-\lg\sigma'_v$  curves. It is observed that the values of  $k_d/k_{ind}$  exhibit a large  
59 scatter. However, most of them are close to unity (mostly from 0.5 to 1.1). This suggests that  
60 at this stage, the indirect method is reasonably valid. Nevertheless, in the case where very high  
61 stress is applied and the soil compressibility changed to very small value,  $k_d/k_{ind}$  turns to be  
62 much larger than unity (Fig. 1b,c), suggesting that the indirect method becomes less valid.  
63 Further examination of Eq. 1 shows that the reliability of indirect value  $k$  mainly depends on  
64 the accuracy of  $c_v$  and  $m_v$ . As pointed out by Tavenas et al. (1979), clays in the normally  
65 consolidated state exhibit significant variations in terms of  $c_v$  and  $m_v$  with changes in void ratio.  
66 This is confirmed by the results of three bentonite specimens shown in Fig. 2 and Fig. 3: a  
67 decreasing trend is identified for  $c_v$  (Fig. 2) and  $m_v$  (Fig. 3). Tavenas et al. (1983) also reported  
68 that the reduction of  $c_v$  near the drainage boundary is much faster than in other part of specimen.  
69 Obviously, this finding is contradictory to the assumption of constant  $c_v$  at each loading step.  
70 Thereby, the indirect value  $k$  is affected by this assumption, explaining the fluctuation observed  
71 in Fig. 1a.

72

73 As the consolidation process steps into the low-compressibility zone, small strain is recorded  
74 and the variations in  $c_v$  and  $m_v$  become moderate (Figs. 2 and 3). These observations are more  
75 consistent with the Terzaghi's assumptions, theoretically making this theory more applicable  
76 in this zone. However, it is observed that  $k_d/k_{ind}$  starts to be larger than unity (see Fig. 1b,c). It  
77 is commonly admitted that in this zone all macro-pores have collapsed and further loading gives  
78 rise to compression of well orientated face-to-face particles. In such orientated microstructure,

79 the physic-chemical interaction between clay particles and absorbed water is enhanced and  
80 starts to govern the global volume change behaviour of specimen (Cui et al., 2013). Mesri and  
81 Olson (1971) also pointed out that while investigating the hydraulic conductivity of soils, it is  
82 important to consider not only the mechanical variables (mainly the size, shape and geometrical  
83 arrangement of the clay particles), but the physico-chemical variables (surface charge density  
84 and distribution, valence of the adsorbed cations as well as the properties of the involved fluid).  
85 From this point of view, the stress induced by the physico-chemical interactions should be  
86 accounted for when calculating the effective stress, which could impact the determination of  $m_v$   
87 by Eq. 2.

88

### 89 **Introduction of a modified effective stress in the indirect method**

90 For saturated soils subjected to an external loading, Terzaghi (1936) introduced an effective  
91 stress in form of Eq.3 and stated that mechanical responds, such as compression, distortion and  
92 changes in shearing resistance, etc., are exclusively due to changes in effective stress:

$$93 \quad \sigma' = \sigma_t - u_w \quad (3)$$

94 where  $\sigma'$  is the effective stress ( $\text{ML}^{-1}\text{T}^{-2}$ ),  $\sigma_t$  is the total external stress ( $\text{ML}^{-1}\text{T}^{-2}$ ) and  $u_w$  is the  
95 pressure ( $\text{ML}^{-1}\text{T}^{-2}$ ) of the free bulk water.

96

97 However, for expansive clayey soils, in addition to free pore water, there are another two kinds  
98 of water: 1) crystalline water which is strongly adsorbed and attached to clay sheets; 2) double  
99 layer water which is well adsorbed to clay particles. Under mechanical loading, free pore water  
100 was compressed, generating pore water pressure. The dissipation of such pressure leads to the  
101 volume change of soil and this process is commonly known as soil consolidation. However, for  
102 the adsorbed water, the changes of its pressure is controlled by the physico-chemical  
103 interactions between the bound water around clay particles and this pressure is interparticle  
104 distance-independent.

105



106 Depending on the circumstances, these two kinds of water pressure could act separately or  
107 together to control the volumetric behaviour of clayey soils. In a consolidating clay with high  
108 compressibility, a large number of large pores exist and the drainage of “free” water in the large  
109 pores is responsible for the volume change. This is accompanied by the development of  
110 particles reorientation and thus the progressive enhancement of physico-chemical interactions  
111 between bound water and clay particles (Bolt, 1956; Mašín and Khalili, 2015); as the  
112 consolidation keeps proceeding in the low compressibility zone, the large pores disappear as all  
113 clay particles are normally well orientated, the “free” water is thoroughly drained out and all  
114 water can be considered as adsorbed water. Thus, the common pore water pressure can be taken  
115 equal to zero and the physico-chemical effects will control the response of the dense clay to  
116 applied loading. However, water can still flow under very high gradients (Pusch et al., 1987).  
117 In such case, the physico-chemical stress can be taken equal to the swelling pressure (Zhang,  
118 2017).

119  
120 Sridharan and Rao (1973) suggested accounting the electrical forces acting in the water-films  
121 around clay particles into the common Terzaghi’s effective stress equation. Lambe (1960)  
122 included the electrical attractive and repulsive forces between water-films around clay particles  
123 as follows:

$$124 \quad \sigma' = \sigma_s + R - A \quad (4)$$

125 where  $\sigma_s$  is the mineral to mineral contact stress ( $\text{ML}^{-1}\text{T}^{-2}$ ),  $R$  is the total interparticle repulsion  
126 divided by total interparticle area ( $\text{ML}^{-1}\text{T}^{-2}$ ),  $A$  is the total interparticle attraction divided by  
127 total interparticle area ( $\text{ML}^{-1}\text{T}^{-2}$ ).  $R-A$  is a general term representing all possible attractive and  
128 repulsive stresses between clay particles.

129  
130 By examining the effective stress in a stiff indurated clay rock theoretically and experimentally,  
131 Zhang (2017) concluded that in a dense clay-water system, the effective stress is transferred

132 through the solid-solid contact between non-clay mineral grains and for the most part, the bound  
 133 pore water in narrow pores, i.e.:

$$134 \quad \sigma' = \sigma_s + \sigma_l \quad (5)$$

135 where  $\sigma_l$  represents the average net repulsive force acting on the bound water-film area divided  
 136 by the total cross-sectional area ( $\text{ML}^{-1}\text{T}^{-2}$ ). The experimental results of Zhang (2017) suggested  
 137 that for stiff indurated clay rock, the swelling pressure is almost equal to the effective stress.  
 138 Mašín and Khalili (2015) referred the net electrical stress acting on water-films between clay  
 139 particles as  $\sigma^{R-A}$  and argued that this kind of stress mainly controls the mechanical behaviour of  
 140 soils with prevailing face-to-face particle arrangement. In this regard, the  $\sigma_l$  and  $\sigma^{R-A}$  refer to the  
 141 same kind of stresses acting in the dense clay-water system.

142

143 Therefore, for the low-compressibility zone where the particle arrangement is dominated by the  
 144 face-to-face feature, the term  $\Delta\sigma_v'$  in Eq. 2 should be revisited. At each loading step the  $\sigma^{R-A}$  is  
 145 assumed to be equal to the swelling pressure  $P_s$  at the corresponding density. The vertical  
 146 effective stress  $\sigma'_{v,i}$  at a given step  $i$  is determined by subtracting the  $P_{s,i}$  value from the applied  
 147 vertical stress  $\sigma_{v,i}$  based on Eq. 6. Then, a new  $m'_{v,i}$  is determined using the modified  $\sigma'_v$  following  
 148 Eq. 7. Thus, a modified indirect value  $k'_{ind}$  can be further calculated by substituting the new  $m'_{v,i}$   
 149 in Eq. 1. With such modifications, the new  $k'_{ind}$  is expected to be closer to the direct value.

$$150 \quad \sigma'_{v,i} = \sigma_{v,i} - P_{s,i} \quad (6)$$

$$151 \quad m'_{v,i} = \frac{\Delta e_i}{(\sigma'_{v,i} - \sigma'_{v,i-1})(1 + e_{i-1})} \quad (7)$$

152

153 It is worth noting that the modification is proposed by incorporating the physico-chemical  
 154 effects into the effective stress equation for dense expansive clays. In other words, the proposed  
 155 approach is an extension of Terzaghi's consolidation theory.

## 156 **Complementary experiment**

157 To evaluate the validity of the proposed modification, an oedometer test was performed on  
158 GMZ bentonite slurry. The bentonite, originated from Inner Mongolia, China, is a Na<sup>+</sup> bentonite  
159 with a montmorillonite fraction of 75.4%. The total cation exchange capacity is 77.30 meq/100g  
160 with 43.36, 29.14, 12.33 and 2.51 meq/100g for Na, Ca, Mg and K, respectively. The bentonite  
161 powder, with particles smaller than 0.2 mm and a solid particles density of 2.66 Mg/m<sup>3</sup>, has a  
162 liquid limit of 276% and a plastic limit of 37%.

163

164 The slurry was prepared by mixing de-aired distilled water with the bentonite powder to reach  
165 a water content of 1.5 times its liquid limit. Care was taken to avoid trapping air bubbles inside.  
166 After 24 h sealing for water homogenization, the slurry was carefully poured into the oedometer  
167 cell with 50 mm inner diameter to the marked height of 30 mm. The oedometer has a steel  
168 porous disk and a filter paper previously placed at the base. Afterwards, a saturated filter paper,  
169 a steel porous disk and the piston were placed at the top of the specimen in sequence. The slurry  
170 was allowed to pre-consolidate under a stress of 0.013 MPa, which corresponds to the piston  
171 weight. The positions of the piston during the pre-consolidation were monitored using a  
172 cathetometer to determine the void ratio change.

173

174 When the pre-consolidation was completed, the oedometer cell was placed in a high-pressure  
175 load frame, which enables a maximum vertical pressure of 50 MPa to be applied on the  
176 specimen. More details about this loading system can be found in Ye et al. (2012). Conventional  
177 step loading was applied with ultimate load equal to 41.25 MPa.

178

179 The values of the coefficient of consolidation  $c_v$  at the last three consolidation steps, where  
180 specimen was expected to be in the low-compressibility zone, were estimated using  
181 Casagrande's method for indirectly determining the hydraulic conductivity. Constant head

182 permeability tests were also carried out after consolidation completion at these three steps under  
183 1 MPa water injection pressure, by using a volume/pressure controller connected to the  
184 oedometer cell. In addition, swelling pressure tests using constant-volume method were  
185 performed on statically compacted GMZ bentonite specimens with void ratios taken from the  
186 compression curve.

### 187 **Application to existing data**

188 The attempts of introducing a modified effective stress into the indirect method are made on  
189 the tested GMZ bentonite slurry, as well as three bentonites in the low-compressibility zone  
190 from literatures. Results are summarized in Table 2 and graphically shown in Fig. 4. It is worth  
191 noting that the values of swelling pressure  $P_s$  of GMZ bentonite were deduced from the swelling  
192 pressure-dry density relationship determined by Ye et al. (2007), while those for Kunigel and  
193 Fourges bentonites were deduced from the correlations established by Wang et al. (2012) based  
194 on the literature data. All these swelling pressure-dry density expressions are given in Table 2.  
195 As expected, since the external stress is partially supported by the physico-chemical forces  
196 between inter-particles, the modified compressibility coefficient  $m'_v$  increases as less  
197 incremental stress is required to cause a certain decrease in void ratio in each loading step  
198 according to Eqs. 6 and 7. In other words, from the perspective of permeability, as compared  
199 to the circumstance before modification, it is easier for the specimen in loading step  $i$  to drain  
200 water with volume change of  $\Delta e_i$  since less incremental effective stress is needed. Therefore,  
201 the modified indirect value  $k'_{ind}$  increases and becomes much closer to the direct value  $k_d$ , making  
202 a significant decrease of  $k_d/k'_{ind}$  ratio. This, in turn, supports the idea of  $\sigma^{R-A} = P_s$  in the case of  
203 compression of orientated face-to-face particles. Note that parameter  $c_v$  is determined based on  
204 the settlement-time curves at each loading step using the common Casagrande method. As  
205 negligible free water is expected to be involved in the low-compressibility zone, the  
206 consolidation process must mainly depend on adsorbed water, thus physically much more  
207 complicated. However, as the void ratio changes a little in this zone, the values of  $c_v$  should

208 change a little too. This is evidenced by the similar  $c_v$  values at different stresses for a given  
209 soil in Table 2. Further examination shows that the improvement of  $k_d/k_{ind}$  results of GMZ  
210 bentonite, range from 1.2 to 1.9, is more significant than that of other soils ranging from 1.7 to  
211 3.8 (Table 2). It is normally due the different accuracies of obtaining swelling pressures: tested  
212 on compacted specimens for GMZ bentonite slurry, deduced from different expressions by Ye  
213 et al. (2007) for compacted GMZ bentonite and Wang et al. (2012) for the rest two slurries.  
214 Furthermore, it is important to note that the swelling pressures used for the three slurries are  
215 determined/estimated from the experiments on compacted soils. As for GMZ bentonite, better  
216 improvement in  $k_d/k_{ind}$  is found in the compacted specimens than the slurry ones (see also Table  
217 2), indicating the idea that in highly compacted bentonite, the net stress  $\sigma^{R-A}$  acting on water-  
218 films between clay particles is equal to its swelling pressure, also, the necessity of determining  
219 the  $\sigma^{R-A}$  in slurry at different void ratios. Better results of  $k_d/k_{ind}$  are expected when the  $\sigma^{R-A}$  is  
220 obtained with the soils tested in slurry state.

221

## 222 **Conclusions**

223 The data of hydraulic conductivity  $k$  of undisturbed, remoulded and compacted expansive soils,  
224 determined in the laboratory by direct and indirect methods are collected and compared,  
225 showing that in the primary compression zone which is characterised by a high compressibility  
226 the two methods give similar results, while in the low-compressibility zone the indirect method  
227 gives much lower hydraulic conductivity.

228

229 In the low-compressibility zone,  $c_v$  is found to be almost constant and the difference between  
230 the direct and indirect methods is attributed to the effect of physic-chemical interaction. The  
231 results of the first attempt with consideration of a modified effective stress accounting for such  
232 interaction show that much closer hydraulic conductivity can be obtained between the direct  
233 and indirect methods, showing the relevance of such an approach.

234

235 It is worth noting that while directly measuring the hydraulic conductivity ( $k_d$ ), there must be a  
236 certain range of error in the test results even though the test is carried out by strictly following  
237 the testing standards. However, as the data obtained here are quite rich, showing the same  
238 variation trend, it is believed that this kind of test error does not affect the general conclusion  
239 drawn in this paper. More data about more expansive clays are of course needed to further  
240 verify this approach.

241

## 242 **Acknowledgements**

243 The authors wish to acknowledge the support of the European Commission by the Marie  
244 Skłodowska-Curie Actions HERCULES - Towards Geohazards Resilient Infrastructure Under  
245 Changing Climates (H2020-MSCA-RISE-2017, 778360) and Shanghai Pujiang Talent  
246 Program (18PJ1410200).

247

## 248 **References**

249 ASTM, 1993. D5856: Standard Test Method for Measurement of Hydraulic Conductivity of  
250 porous material using a rigid-wall, Compaction-mold Permeameter. ASTM International,  
251 West Conshohocken, PA, USA.

252 ASTM, 2010. D5084: Standard test methods for measurement of hydraulic conductivity of  
253 saturated porous materials using a flexible wall permeameter. ASTM International, West  
254 Conshohocken, PA, USA.

255 ASTM, 2011. D7100: Standard Test Method for Hydraulic Conductivity Compatibility Testing  
256 of Soils with Aqueous Solutions. ASTM International, West Conshohocken, PA, USA.

257 Bolt, G.H., 1956. Physico-chemical analysis of the compressibility of pure clays. *Géotechnique*,  
258 6(2), 86-93.

259 Casagrande, A., and Fadum, R.E. 1944. Reply to discussions on Application of soil mechanics  
260 in designing building foundations. ASCE Transaction Paper, No. 2213, 383-490.

261 Cui, Y.J., Nguyen, X.P., Tang, A.M., Li, X.L. 2013. An insight into the unloading/reloading  
262 loops on the compression curve of natural stiff clays. *Applied Clay Science*, 83: 343-348.  
263 doi:10.1016/j.clay.2013.08.003.

264 Daniel, D.E. 1994. State-of-the-art: Laboratory hydraulic conductivity tests for saturated soils.  
265 Hydraulic conductivity and waste contaminant transport in soil. ASTM STP 1142, David  
266 E Daniel and Stephen J Trautwein, Eds., ASTM, Philadelphia.

267 Deng, Y.F., Cui, Y.J., Tang, A.M., Nguyen, X.P., Li, X.L., Greet, M.V. 2011. Investigating the  
268 pore-water chemistry effects on the volume change behaviour of Boom clay. *Physics and  
269 Chemistry of the Earth, Parts A/B/C*, 36(17): 1905-1912. doi:10.1016/j.pce.2011.07.016.

- 270 Lambe, T.W. 1960. A mechanistic picture of shear strength in clay. In Research conference on  
271 shear strength of cohesive soils, ASCE, 555-580.
- 272 Malusis, M.A., Barben, E.J. and Evans, J.C. 2009. Hydraulic conductivity and compressibility  
273 of soil-bentonite backfill amended with activated carbon. *Journal of geotechnical and*  
274 *geoenvironmental engineering*, 135(5): 664-672. doi:10.1061/(ASCE)GT.1943-  
275 5606.0000041
- 276 Marcial, D., Delage, P. and Cui, Y.J. 2002. On the high stress compression of bentonites.  
277 *Canadian Geotechnical Journal*, 39(4): 812-820. doi: 10.1139/T02-019.
- 278 Mašín, D. and Khalili, N. 2015. Swelling phenomena and effective stress in compacted  
279 expansive clays. *Canadian Geotechnical Journal*, 53(1): 134-147. doi:10.1139/cgj-2014-  
280 0479.
- 281 Mesri, G. and Olson, R.E. 1971. Mechanisms controlling the permeability of clays. *Clays and*  
282 *Clay Minerals*, 19(3): 151-158. doi: 10.1346/CCMN.1971.0190303.
- 283 Mesri G., Feng, T.W., Ali, S., Hayat, T.M. 1994. Permeability characteristics of soft clays.  
284 *Proc. of the 13<sup>th</sup> Int. Conf. on Soil Mechanics and Foundation Engineering*, Vol 2, Japanese  
285 *Society of Soil Mechanics and Foundation Engineering*, Tokyo, 187-192.
- 286 Mesri, G. and Funk, J.R. 2015. Settlement of the kansai international airport islands. *Journal of*  
287 *Geotechnical and Geoenvironmental Engineering*, 141(2): 04014102.  
288 doi:10.1061/(ASCE)gt.1943-5606.0001224.
- 289 Nguyen, X.P., Cui, Y.J., Tang, A.M., Deng, Y.F., Li, X.L., Wouters, L. 2013. Effects of pore  
290 water chemical composition on the hydro-mechanical behavior of natural stiff clays.  
291 *Engineering Geology*, 166: 52-64. B.V. All rights reserved.  
292 doi:10.1016/j.enggeo.2013.08.009
- 293 Pusch, R., Hokmark, H., and Borgesson, L., 1987. Outline of models of water and gas flow  
294 through smectite clay buffers. SKB Technical Report 87-10.
- 295 Retnamony, G.R., Robinson, R.G. and Allam, M.M. 1998. Effect of clay mineralogy on  
296 coefficient of consolidation. *Clays and clay minerals*, 46(5): 596-600.  
297 doi:10.1346/CCMN.1998.0460514
- 298 Sridharan, A. and Nagaraj, H.B. 2004. Coefficient of consolidation and its correlation with  
299 index properties of remolded soils. *Geotechnical Testing Journal*, 27(5): 469-474.
- 300 Sridharan, A. and Rao, G.V. 1973. Méchanisms controlling volume change of saturated clays  
301 and the role of the efective stress concept. *Géotechnique*, 23(3): 359-382.  
302 doi:10.1680/geot.1973.23.3.359
- 303 Terzaghi, K. 1936. The shearing resistance of saturated soils and the angle between the planes  
304 of shear. In *International Conference on Soil Mechanics and Foundation Engineering*, pp.  
305 54–56. Harvard University Press: Cambridge, MA.
- 306 Taylor, D.W. 1948. *Fundamentals of soils mechanics*. John Wiley, New York.

- 307 Tavenas, F., Brucy, M., Magnan, J.P., La Rochelle, P., Roy, M. 1979. Analyse critique de la  
308 théorie de consolidation unidimensionnelle de Terzaghi. *Revue Française Géotechnique*,  
309 (7): 29-43.
- 310 Tavenas, F., Leblond, P., Jean, P., Leroueil, S. 1983. The permeability of natural soft clays. Part  
311 I: Methods of laboratory measurement. *Canadian Geotechnical Journal*, 20(4): 629-644.  
312 doi:10.1139/t83-072.
- 313 Wang, Q., Tang, A.M., Cui, Y.J., Delage, P., Gatmiri, B. 2012. Experimental study on the  
314 swelling behaviour of bentonite/claystone mixture. *Engineering Geology*, 124: 59-66.  
315 doi:10.1016/j.enggeo.2011.10.003.
- 316 Watabe, Y., Yamada, K. and Saitoh, K. 2011. Hydraulic conductivity and compressibility of  
317 mixtures of Nagoya clay with sand or bentonite. *Géotechnique*, 61(3): 211-219.  
318 doi:10.1680/geot.8.P.087
- 319 Ye, W.M., Schanz, T., Qian, L.X., Wang, J., Arifin 2007. Characteristics of swelling pressure of  
320 densely compacted Gao-Mao-Zi bentonite GMZ01. *Chinese Journal of Rock and  
321 Mechanics and Engineering*, 26(2): 3861-3865.
- 322 Ye, W.M., Zhang, Y.W., Chen, B., Chen, Y.G., Zheng, Z.J., Cui, Y.J. 2012. Investigation on  
323 compression behaviour of highly compacted gmz01 bentonite with suction and  
324 temperature control. *Nuclear Engineering & Design*, 252: 11-18. doi:  
325 10.1016/j.nucengdes.2012.06.037.
- 326 Ye, W.M., Zhang, F., Chen, B., Chen, Y.G., Wang, Q., Cui, Y.J. 2014. Effects of salt solutions  
327 on the hydro-mechanical behavior of compacted GMZ01 Bentonite. *Environmental earth  
328 sciences*, 72(7): 2621-2630. doi:10.1007/s12665-014-3169-x.
- 329 Zhang, C.L. 2017. Examination of effective stress in clay rock. *Journal of Rock Mechanics and  
330 Geotechnical Engineering*, 9(3): 479-489. doi:10.1016/j.jrmge.2016.07.008.
- 331 Zhu, C.M., Ye, W.M., Chen, B., Chen, Y.G., Cui, Y.J. 2013. Influence of salt solutions on the  
332 swelling pressure and hydraulic conductivity of compacted GMZ01 bentonite.  
333 *Engineering Geology*, 166: 74-80. doi: 10.1016/j.enggeo.2013.09.001.



334 **List of Tables**

335 Table 1. Main information of consolidation-permeability tests from the literature

336 Table 2. Information of indirect  $k$  before and after modification

337 **List of Figures**

338 Figure 1. Evolution of  $k_d/k_{ind}$  during consolidation, together with the compression curves; (a)  
339 slurry in the loading range from 1-2000 kPa, (b) slurry in the loading range from 0.001-100  
340 MPa, (c) compacted and undisturbed clays in the loading range from 0.01-100 MPa

341 Figure 2. Evolution of  $c_v$  during consolidation of three bentonites, together with the  
342 compression curves; (a) compacted GMZ bentonite, (b) Kunigel bentonite slurry and Fourges  
343 slurry

344 Figure 3. Evolution of  $m_v$  together with the compression curves; (a) compacted GMZ bentonite,  
345 (b) Kunigel bentonite slurry and Fourges slurry

346 Figure 4. Comparisons of  $k_{ind}$  and modified  $k'_{ind}$ , together with the compression curves; (a) GMZ  
347 bentonite, (b) Kunigel bentonite slurry and Fourges slurry

348

349 Table 1. Main information of consolidation-permeability tests from the literature

<i>Type</i>	<i>Soil</i>	<i>w<sub>L</sub></i>	<i>Loading range</i>	<i>c<sub>v</sub> determination method</i>	<i>Permeability test</i>	<i>Reference</i>
Slurry	Kunigel bentonite	474%	0.13-30 MPa	Casagrande's	constant-head	Marcial et al. (2002)
	Fourges clay	112%				
	Carbon-amended bentonite-sand	27%-42%	24-1532 kPa	Casagrande's	falling-head	Malusis et al. (2009)
	Nagoya clay-sand	/	9.8-1256 kPa	Taylor's	falling-head	Watabe et al. (2011)
	Nagoya clay-bentonite	/				
Undisturbed soil	Boom clay	67.2%	0.05-3.2 MPa	Casagrande's	constant-head	Deng et al. (2010)
	Boom clay	67.2%	0.05-3.2 MPa	Casagrande's	constant-head	Ngyuen et al. (2013)
Compacted soil	GMZ bentonite	276%	0.5-42 MPa	Casagrande's	constant-head	Zhu et al. (2013)
						Ye et al. (2014)

350

351 Table 2. Information of indirect  $k$  before and after modification

Soil	$e$	$\sigma_v'$ (MPa)	$P_s$ (MPa)	Modified $\sigma_v'$ (MPa)	$c_v$ (m <sup>2</sup> /s)	$m_v$ (kPa <sup>-1</sup> )	$m_v'$ (kPa <sup>-1</sup> )	$k_d$ (m/s)	$k_{ind}$ (m/s)	$k_{ind}'$ (m/s)	$k_d / k_{ind}$	$k_d / k_{ind}'$	Data resource
GMZ	0.64	11.57	3.67	7.90	/	/	/	/	/	/	/	/	
bentonite	0.52	17.32	7.12	10.20	7.1×10 <sup>-10</sup>	1.2×10 <sup>-5</sup>	3.0×10 <sup>-5</sup>	2.4×10 <sup>-13</sup>	8.4×10 <sup>-14</sup>	2.1×10 <sup>-13</sup>	2.9	1.2	this work
slurry	0.46	29.29	14.90	14.39	9.7×10 <sup>-10</sup>	3.3×10 <sup>-6</sup>	9.5×10 <sup>-6</sup>	1.2×10 <sup>-13</sup>	3.2×10 <sup>-14</sup>	9.3×10 <sup>-14</sup>	3.6	1.3	
	0.42	41.25	22.75	18.50	6.5×10 <sup>-10</sup>	3.9×10 <sup>-6</sup>	7.6×10 <sup>-6</sup>	9.2×10 <sup>-14</sup>	2.6×10 <sup>-14</sup>	4.9×10 <sup>-14</sup>	3.6	1.9	
Compacted	0.74	5.21	1.66	3.55	1.6×10 <sup>-9</sup>	1.8×10 <sup>-5</sup>	2.5×10 <sup>-5</sup>	5.8×10 <sup>-13</sup>	3.0×10 <sup>-13</sup>	4.8×10 <sup>-13</sup>	2.0	1.2	Zhu et al (2013)
GMZ	0.54	20.98	7.49	13.49	1.2×10 <sup>-9</sup>	5.9×10 <sup>-6</sup>	9.8×10 <sup>-6</sup>	2.1×10 <sup>-13</sup>	8.3×10 <sup>-14</sup>	1.4×10 <sup>-13</sup>	2.5	1.5	Ye et al (2014)
bentonite	0.47	38.42	13.39	25.03	1.6×10 <sup>-9</sup>	2.5×10 <sup>-6</sup>	3.8×10 <sup>-6</sup>	1.1×10 <sup>-13</sup>	4.8×10 <sup>-14</sup>	7.2×10 <sup>-14</sup>	2.3	1.5	
Kunigel	0.47	8.38	2.03	6.35	6.7×10 <sup>-11</sup>	1.4×10 <sup>-5</sup>	1.7×10 <sup>-5</sup>	3.1×10 <sup>-14</sup>	9.7×10 <sup>-15</sup>	1.3×10 <sup>-14</sup>	3.2	2.3	Marcial et al (2002)
bentonite	0.32	31.23	4.09	27.14	1.0×10 <sup>-10</sup>	1.4×10 <sup>-6</sup>	1.5×10 <sup>-6</sup>	6.4×10 <sup>-15</sup>	1.5×10 <sup>-15</sup>	1.9×10 <sup>-15</sup>	4.3	3.4	
Fourges	0.82	8.38	0.59	7.79	4.8×10 <sup>-10</sup>	2.0×10 <sup>-5</sup>	2.2×10 <sup>-5</sup>	2.0×10 <sup>-13</sup>	9.8×10 <sup>-14</sup>	1.3×10 <sup>-13</sup>	2.5	1.6	
clay	0.74	16.59	1.17	15.42	4.9×10 <sup>-10</sup>	5.9×10 <sup>-6</sup>	6.3×10 <sup>-6</sup>	1.4×10 <sup>-13</sup>	2.9×10 <sup>-14</sup>	3.8×10 <sup>-14</sup>	4.2	3.8	
	0.65	31.23	2.51	28.72	5.3×10 <sup>-10</sup>	3.5×10 <sup>-6</sup>	3.8×10 <sup>-6</sup>	4.1×10 <sup>-14</sup>	1.9×10 <sup>-14</sup>	2.5×10 <sup>-14</sup>	2.5	1.7	

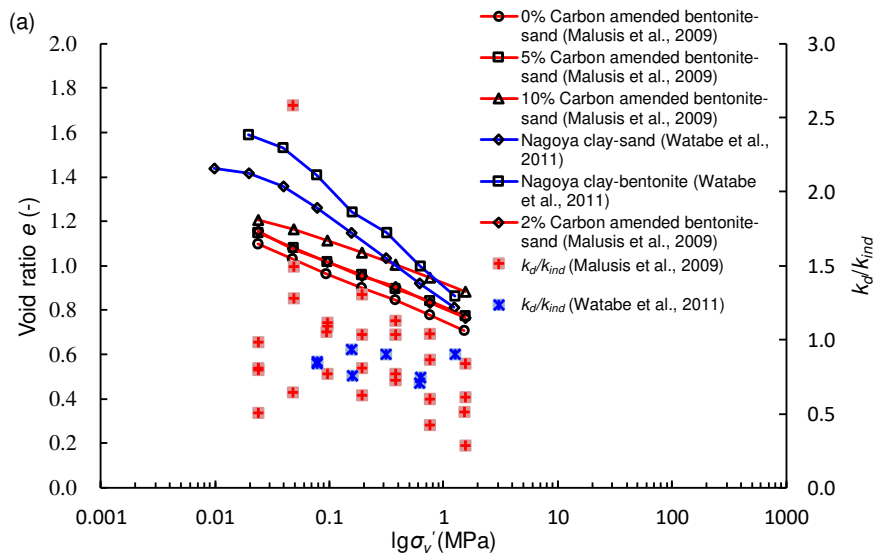
352 \*  $P_s$  of compacted GMZ bentonite from Ye et al (2014) with distilled water is calculated based on the prediction equation by Ye et al. (2007).  $P_s = 1.94 \times 10^{-3} \exp(7.419 \rho_d)$  (MPa), where  $\rho_d$  is the dry density

353 of bentonite (Mg/m<sup>3</sup>).

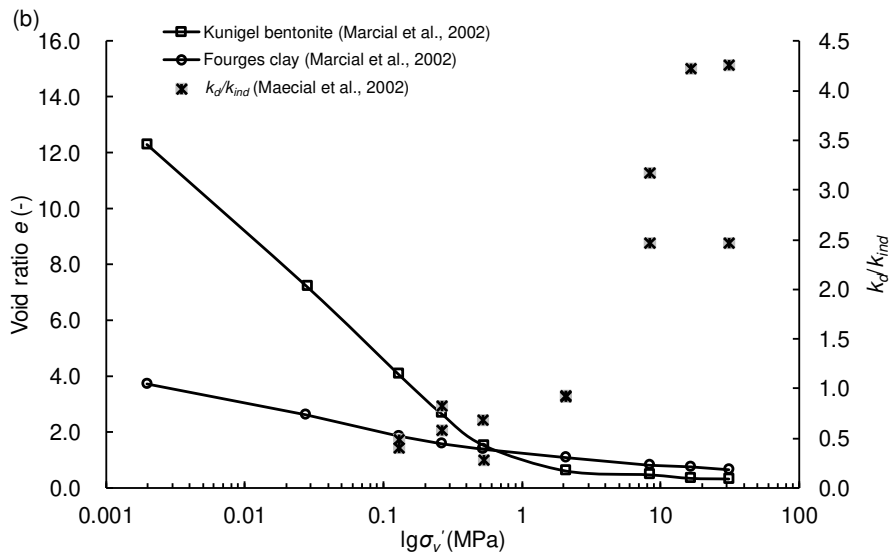
354  $P_s$  of Kunigel and Fourges bentonite are calculated based on the prediction equations by Wang et al. (2012). Kunigel:  $P_s = 3.67 \times 10^{-3} \exp(3.32\rho_d)$ ; Fourges:  $P_s = 7.83 \times 10^{-7} \exp(9.24\rho_d)$ .

355 <sup>a</sup> data from personal communication

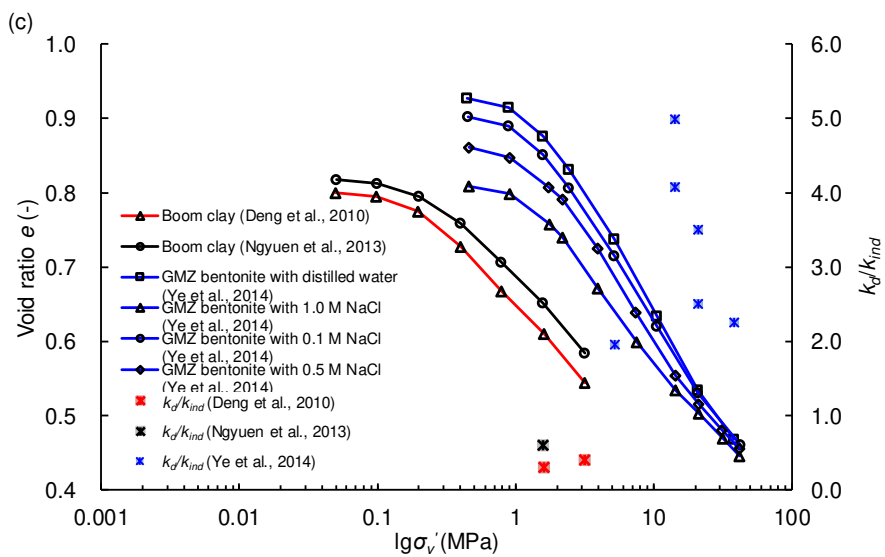
356



357

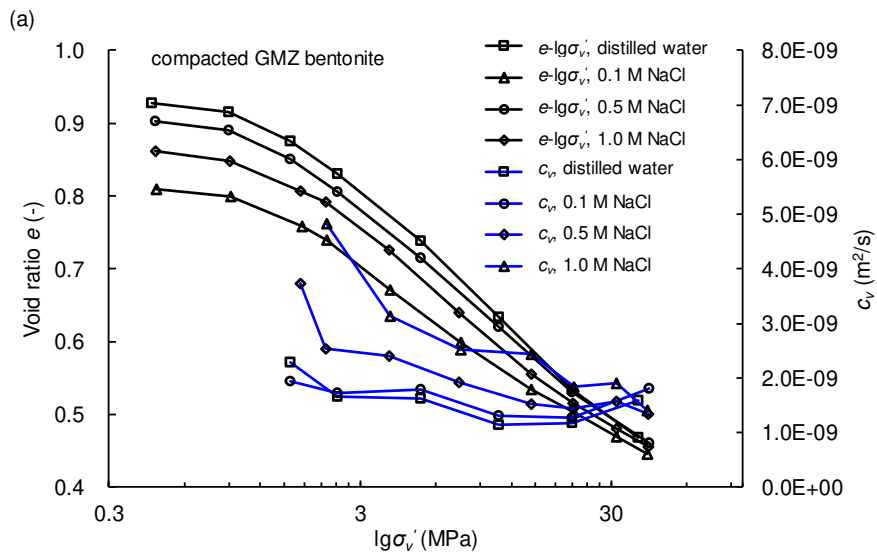


358

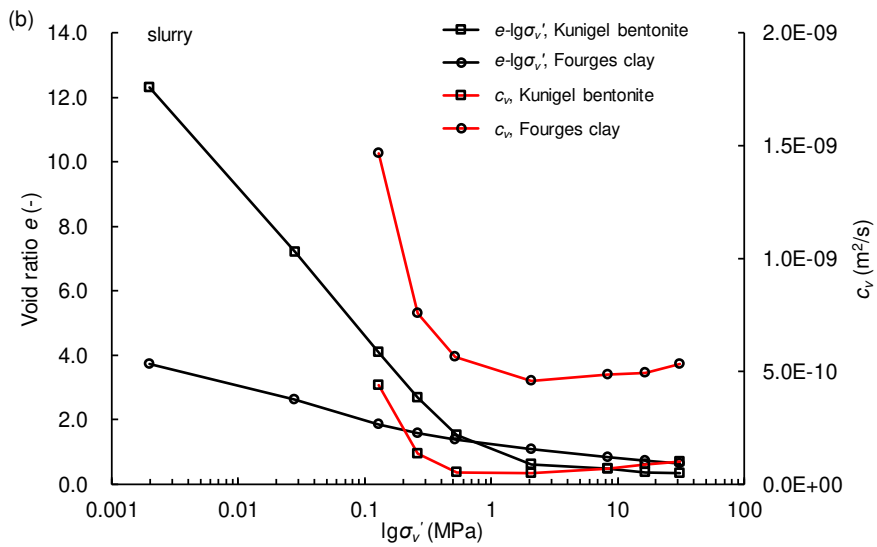


359

360 Figure 1. Evolution of  $k_d/k_{ind}$  during consolidation, together with the compression curves; (a)  
 361 slurry in the loading range from 1-2000 kPa, (b) slurry in the loading range from 0.001-100  
 362 MPa, (c) compacted and undisturbed clays in the loading range from 0.01-100 MPa



363

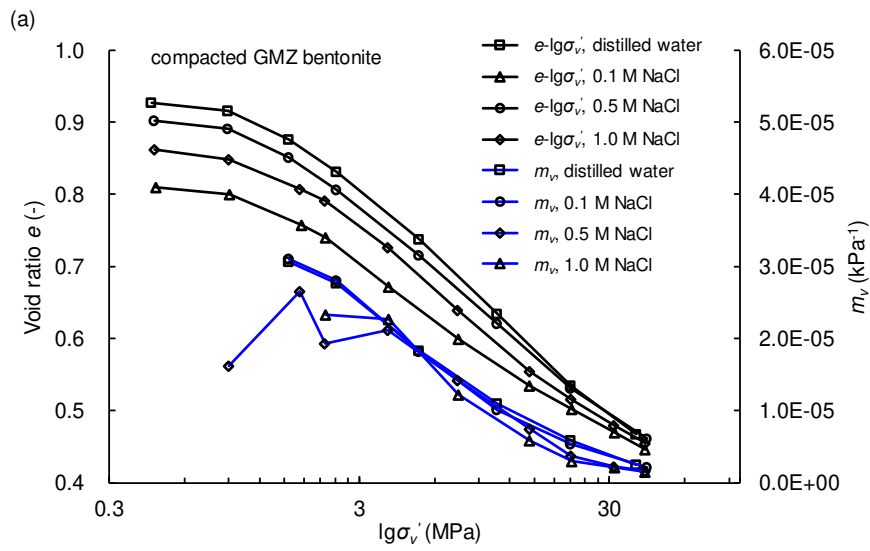


364

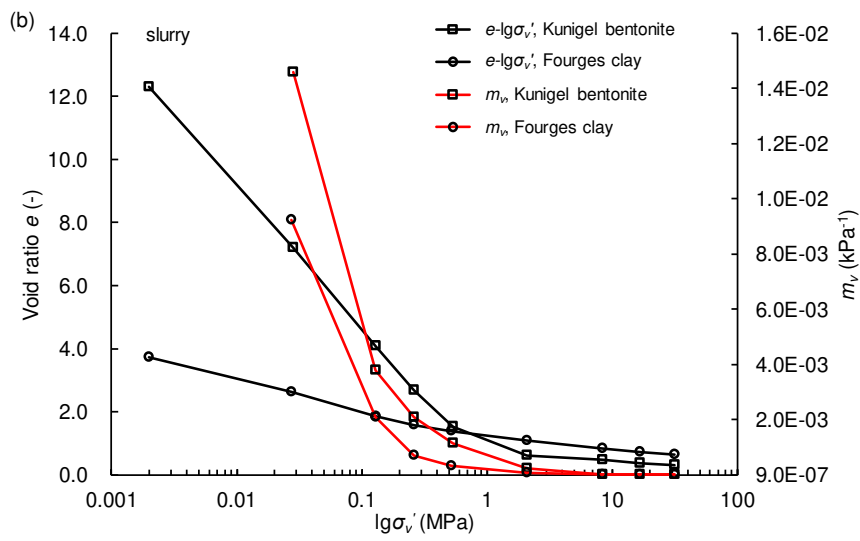
365 Figure 2. Evolution of  $c_v$  during consolidation of three bentonites, together with the  
 366 compression curves; (a) compacted GMZ bentonite, (b) Kunigel bentonite slurry and Fourges  
 367 slurry

368

369



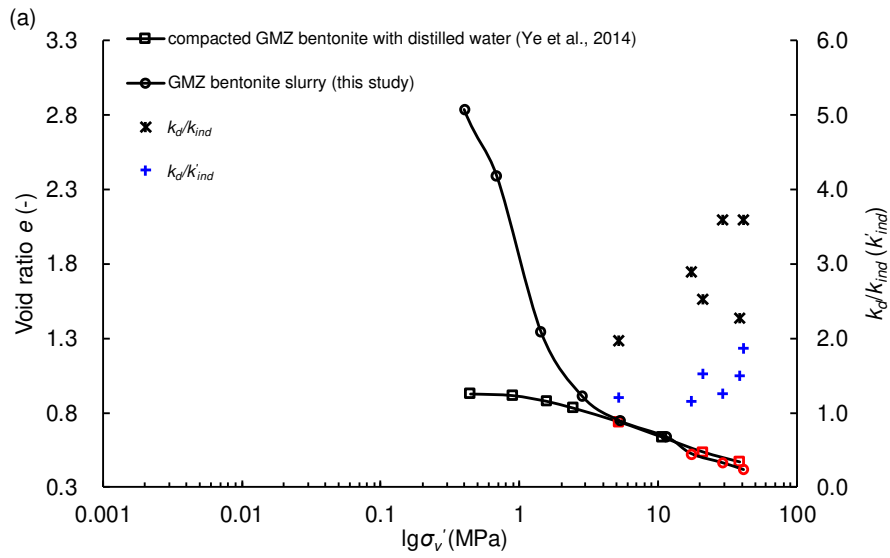
370



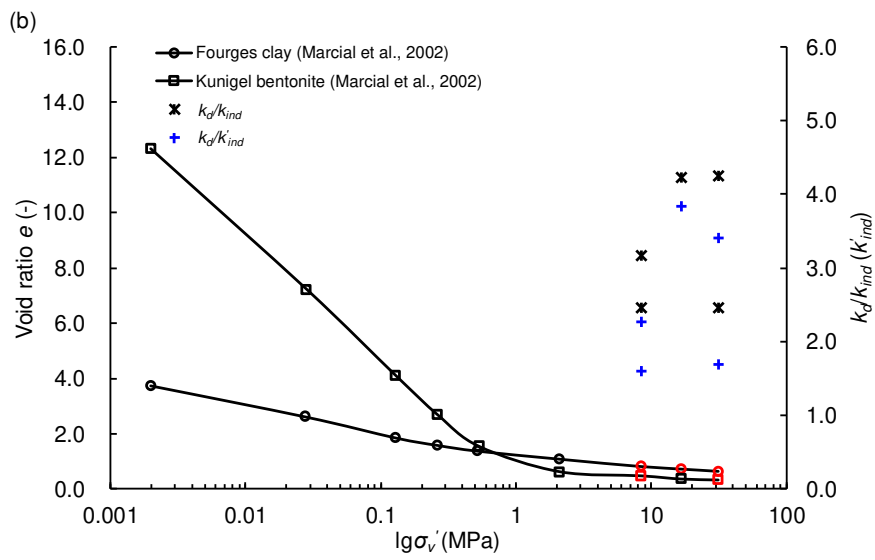
371

372 Figure 3. Evolution of  $m_v$  together with the compression curves; (a) compacted GMZ bentonite,

373 (b) Kunigel bentonite slurry and Fourges slurry



374



375

376 Figure 4. Comparisons of  $k_{ind}$  and modified  $k'_{ind}$ , together with the compression curves; (a) GMZ

377 bentonite, (b) Kunigel bentonite slurry and Fourges slurry